

# Photoinduced Intramolecular Charge Separation in Donor/Acceptor-Substituted Bicyclohexylidene and Bicyclohexyl

Frans J. Hoogesteger,<sup>[a]</sup> Cornelis A. van Walree,<sup>[a]</sup> Leonardus W. Jenneskens,<sup>\*[a]</sup> Martin R. Roest,<sup>[b]</sup> Jan W. Verhoeven,<sup>[b]</sup> Wouter Schuddeboom,<sup>[c]</sup> Jacob J. Piet,<sup>[c]</sup> and John M. Warman<sup>[c]</sup>

**Abstract:** The photophysical properties of a bicyclohexylidene (**1DA**) and a bicyclohexyl (**2DA**) substituted with an anilino electron donor and a dicyanoethylene electron acceptor have been studied. Quenching of local donor emission is observed for these compounds as well as quenching of the “pseudo-local” acceptor emission. Transient absorption spectra show dialkylanilino-type radical-cation and dicyanoethylene-type radical-anion absorptions. These results show that intramolecular charge separation takes place in **1DA** and **2DA**. This

was corroborated by time-resolved microwave conductivity measurements from which large excited-state dipole moments were found for both **1DA** and **2DA**. Time-resolved fluorescence spectroscopy revealed that in the charge-separated state in cyclohexane for **2DA**, molecular folding takes place on a nanosecond timescale. For **1DA** in cyclo-

**Keywords:** electron transfer • laser spectroscopy • synthetic methods • through-bond interactions

hexane, either charge separation takes place in a (fully) folded conformation or very rapid (subnanosecond timescale) folding takes place subsequent to charge separation. In addition to this difference in conformational behavior, the presence of the exocyclic double bond between the cyclohexyl-type rings results in efficient quenching of the anilino donor triplet state and acceleration of the charge recombination rate by a factor of 20.

## Introduction

The occurrence of photoinduced electron-transfer processes has attracted the attention of many researchers, since its study may provide insight into the processes that play a role in the conversion of solar energy into an electrochemical potential in photosynthetic systems.<sup>[1]</sup> In addition, knowledge about these phenomena is of importance for the rational development of new optoelectronic materials that may find an application in the fields of artificial solar-energy conversion,<sup>[2]</sup> nonlinear optics,<sup>[3]</sup> and molecular electronics.<sup>[4]</sup> In order to obtain a better understanding of the factors that govern charge-transfer processes, charge transfer in donor-spacer-acceptor (DSA) compounds that contain a variety of inter-

connecting saturated hydrocarbon spacers has been studied.<sup>[5]</sup> It has been shown that no direct spatial overlap between the donor and acceptor wavefunctions is necessary for the occurrence of charge transfer, since the intervening bridge has a rigid character in several of these systems. In these cases, the interaction between D and A is a result of through-bond orbital interactions. The concept of through-bond interactions (TBI) was introduced in 1968 by Hoffmann et al. and describes the intramolecular interactions between functional groups non-conjugatively linked by orbital overlap.<sup>[6]</sup> Experimental evidence for TBI has been obtained from photoelectron and electronic spectroscopy as well as structural<sup>[7]</sup> and chemical studies.<sup>[8]</sup>

Bi- and oligo(cyclohexylidenes)<sup>[9]</sup> are interesting candidates for use as spacers in DSA compounds, since their alternating  $\sigma$ - $\pi$ - $\sigma$  orbital topology allows the study of the influence of formally nonconjugated double bonds in the bridge on photoinduced charge-transfer phenomena. Ab initio calculations have shown that the  $\pi$  bonds in oligo(cyclohexylidenes) are mutually weakly coupled by orbital interactions.<sup>[10]</sup> They are also sufficiently easy to oxidize to render the intervening bridge “redox active”.<sup>[10]</sup> Thus, the unsaturated entity can be involved in the charge-separation process in two ways.<sup>[2, 11, 12]</sup> Firstly, through TBI it can increase the electronic coupling between donor and acceptor orbitals by providing relatively

[a] Prof. L. W. Jenneskens, Dr. F. J. Hoogesteger, Dr. C. A. van Walree  
Debye Institute, Department of Physical Organic Chemistry  
Utrecht University, Padualaan 8, 3584 CH Utrecht (The Netherlands)  
Fax: (+31) 302534533  
E-mail: jennesk@chem.uu.nl

[b] Dr. M. R. Roest, Prof. J. W. Verhoeven  
Laboratory of Organic Chemistry, University of Amsterdam  
Nieuwe Achtergracht 129, 1018 WS, Amsterdam (The Netherlands)

[c] Dr. W. Schuddeboom, J. J. Piet, Dr. J. M. Warman  
IRI, Delft University of Technology, Mekelweg 15  
2629 JB Delft (The Netherlands)

low-lying, that is, lower than the  $\sigma^*$  orbitals of the saturated bridge, empty  $\pi^*$  orbitals. Secondly, the unsaturated system can function as a real anion or cation intermediate in the electron-transfer process (sequential mechanism). By comparison of the photophysical properties of donor/acceptor-substituted oligo(cyclohexylidenes) with saturated oligo(cyclohexyl) analogues the effect of the  $\pi$  bond on electron-transfer processes can be assessed.

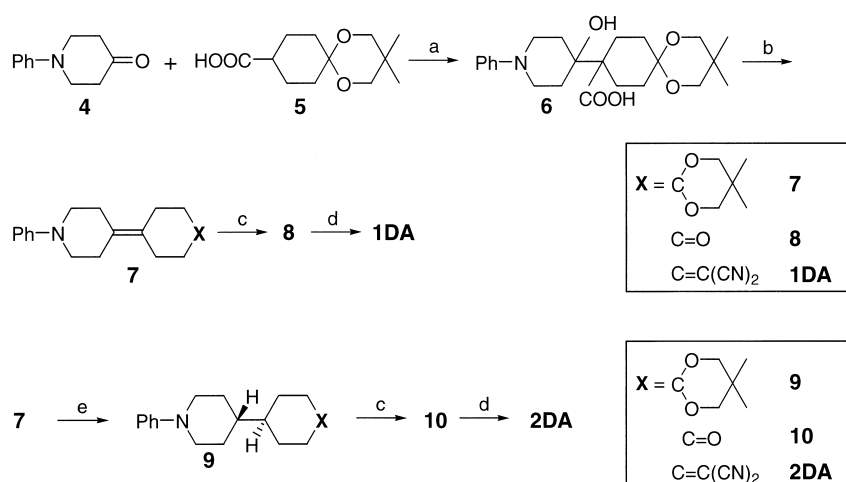
In addition to providing insight into the role of an isolated double bond in charge-separation processes, functionalized oligo(cyclohexylidenes) also offer the possibility of obtaining well-organized optoelectronic materials. It has been shown that the oligo(cyclohexylidene) building block gives access to highly ordered supramolecular structures by using the Langmuir–Blodgett technique, self-complementary hydrogen bonding, and spin-coating.<sup>[13]</sup> Since this tendency to form supramolecular structures is related to the geometry of oligo(cyclohexylidenes), the effect of charge separation on the conformation of these compounds is of interest. Oligo(cyclohexylidenes) in general possess a rodlike geometry<sup>[9a]</sup> that formally prevents a through-space overlap of the D and A chromophores. However, conformational flexibility of the bridge may give rise to a more compact (folded) structure. In a folded ground-state conformation, through-space electron transfer may take place upon excitation (DSA molecules with a polymethylene bridge show this behavior).<sup>[8, 14]</sup> It is also possible that folding occurs subsequent to charge transfer in an extended conformation. This phenomenon is the result of a coulombic attraction between the oppositely charged chromophores at both end-positions of the molecule and is operative in media that have little interaction with the charge-separated state (gas phase or nonpolar solvents). This so-called harpooning mechanism<sup>[15]</sup> has been observed for certain piperidine-bridged DSA systems.<sup>[16]</sup>

In this paper the photophysical properties of a bicyclohexylidene (**1DA**) and a bicyclohexyl (**2DA**) that contain electron-donating anilino groups and electron-accepting dicyanoethylene groups are described. In addition, model donor compounds (**1D**; **2D**) and model acceptor compounds (**1A**; **2A**) are studied. The photophysical properties were inves-

tigated by applying a variety of techniques, including absorption spectroscopy, steady-state and time-resolved (nanosecond timescale) fluorescence spectroscopy, transient absorption (TA) spectroscopy, and time-resolved microwave conductivity (TRMC) measurements. To obtain insight into their conformational behaviour in the ground state, the <sup>1</sup>H NMR spectra of the synthesized compounds are also addressed. It is shown that the presence of a double bond in the D–A-connecting bicyclohexylidene framework has a profound influence on both the conformational and charge-transfer properties of the compounds investigated.

## Results and Discussion

**Synthesis:** The synthesis of compounds **1DA** and **2DA** is shown in Scheme 1. Alkylation of the dianion of carboxylic acid **5** with *N*-phenylpiperidone<sup>[17]</sup> **4** afforded  $\beta$ -hydroxy acid **6**, which was decarboxylated and dehydrated to yield acetal **7**. Hydrolysis of **7** yielded ketone **8** and subsequent condensation

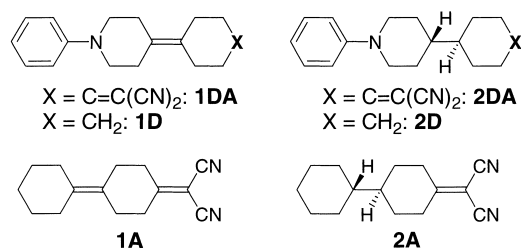


Scheme 1. Synthetic scheme for **1DA** and **2DA**. Reagents: a) BuLi, (*i*Pr)<sub>2</sub>NH; b) Me<sub>2</sub>NCH(OCH<sub>2</sub>CM<sub>3</sub>)<sub>2</sub>, CH<sub>3</sub>CN; c) H<sub>3</sub>O<sup>+</sup>, THF; d) H<sub>2</sub>C(CN)<sub>2</sub>, C<sub>6</sub>H<sub>6</sub>; H<sub>2</sub>, Pd/C, THF.

with malononitrile afforded **1DA**. Saturated compound **2DA** was obtained by catalytic hydrogenation of **7**, followed by hydrolysis to ketone **10**, and condensation with malononitrile.

The synthesis of donor model compound **1D** is straightforward starting from **4** and cyclohexanecarboxylic acid. Catalytic hydrogenation of **1D** afforded **2D**. Acceptor models **1A** and **2A** were obtained by Knoevenagel condensation of malononitrile and 1,1'-bicyclohexylidene-4-one<sup>[9]</sup> and 1,1'-bicyclohexyl-4-one,<sup>[18]</sup> respectively. All donor/acceptor compounds possess high melting points and low solubilities in common organic solvents.<sup>[19]</sup>

**Ground-state conformational properties of 1DA and 2DA:** In principle, due to the possibility of ring inversion, several conformations are accessible for compounds that contain cyclohexyl-type rings. Unfortunately, crystals of the donor/acceptor compounds suitable for X-ray diffraction were not available. However, the single-crystal X-ray structure of ketone **8** has been reported.<sup>[20]</sup> In this compound the cyclo-



hexyl-type rings adopt a chair conformation and the phenyl ring occupies an equatorial position. In the two crystallographically independent molecules in the unit cell the phenyl ring appears to be twisted with respect to the piperidine type ring by 40 and 50°.

<sup>1</sup>H NMR spectroscopy reveals that important conformational differences exist between the bicyclohexylidene (series **1**) and the bicyclohexyl derivatives (series **2**) in solution. The <sup>1</sup>H NMR spectrum of **1D** shows a single triplet at  $\delta = 3.22$  for the four protons adjacent to the nitrogen atom. This indicates that they are isochronous at room temperature and that their neighboring protons are also magnetically equivalent. Indeed, a triplet is also found for the allylic protons ( $\delta = 2.46$ ) of the nitrogen-containing ring. This provides evidence that both cyclohexyl-type ring inversions and nitrogen inversion are rapid on the NMR timescale. A similar conformational mobility behavior is found for **1A**; the four protons adjacent to the dicyanomethylene substituent and the four allylic neighboring protons appear as triplets in the <sup>1</sup>H NMR spectrum. For **1DA**, the aliphatic part of the <sup>1</sup>H NMR spectrum shows patterns for the allylic protons similar to those of **1D** and **1A**. Hence, it is concluded that the compounds containing exocyclic double bonds (**1DA**, **1D**, and **1A**) are conformationally flexible at room temperature on the NMR timescale.

The <sup>1</sup>H NMR spectra of series **2** are much more complex than those of series **1**. Distinct signals are discernible for equatorial and axial protons of the cyclohexyl-type rings. For **2DA**, equatorial and axial protons adjacent to the nitrogen atom resonate at  $\delta = 3.72$  and 2.62, respectively. The upfield shift of the axial protons with respect to the equatorial ones is a consequence of the axial orientation of the nitrogen lone pair. This indicates that the phenyl group occupies an equatorial position in **2DA**.<sup>[21]</sup> Thus, the single bond that connects the two cyclohexyl-type rings effectively locks the conformation of the cyclohexyl rings and the equatorial position of the phenyl group. This observation also applies to **2A**; at room temperature it possesses a frozen conformation on the NMR timescale.

The difference in conformational behavior between series **1** and **2** must find its origin in the presence of an sp<sup>2</sup>-hybridised bridging carbon atom in the series **1**. Upon chair–chair interconversion, in the bicyclohexylidene system only the phenyl group moves to an axial position, whereas in the bicyclohexyl series both a phenyl and a cyclohexyl ring are forced to adopt an axial position. The latter geometry is energetically highly unfavorable, and the equilibrium will be situated at the equatorial–equatorial conformation. Another factor that enhances the conformational mobility of the series **1** is the lowering of the barrier for chair–chair interconversion by an sp<sup>2</sup>-hybridized carbon atom by about 2.5 kcal mol<sup>-1</sup>, which is due to a reduction in the number of repulsive nonbonded H–H interactions.<sup>[22]</sup> It should be emphasized that the observed difference in conformational mobility in the ground state may have important consequences with respect to geometrical changes after photoexcitation (vide infra).

**Absorption spectra:** The UV absorption spectra of **1DA**, **2DA** and their donor (**1D**, **2D**) and acceptor (**1A**,

**2A**) model compounds are shown in Figure 1. Absorption maxima and molar absorption coefficients are summarized in Table 1.

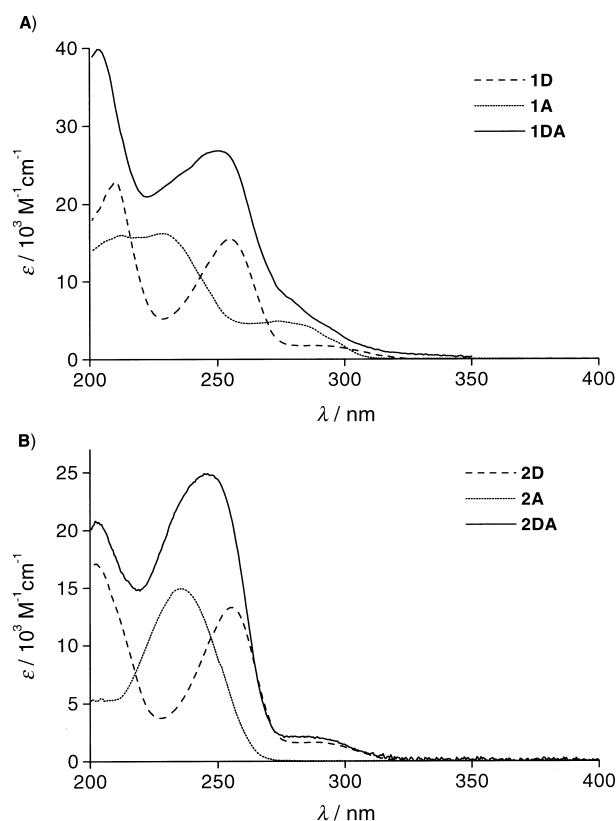


Figure 1. UV absorption spectra of A) **1DA**, **1D** and **1A** and B) **2DA**, **2D** and **2A**. All spectra were recorded in cyclohexane.<sup>[26]</sup>

Table 1. Absorption maxima and molar extinction coefficients  $\epsilon$  (in parentheses) of DA compounds (**1DA**, **2DA**), donor model compounds (**1D**, **2D**), and acceptor model compounds (**1A**, **2A**) in cyclohexane at 20 °C.

	$\lambda_{\max}$ [nm] ( $\epsilon$ [ $10^3 \text{ M}^{-1} \text{ cm}^{-1}$ ])		
<b>1DA</b>	203 (39.8)	251 (26.8)	286 (5.7)
<b>2DA</b>	203 (20.6) <sup>[a]</sup>	245 (25.0) <sup>[a]</sup>	289 (2.3) <sup>[a]</sup>
<b>1D</b>	210 (22.9)	255 (15.5)	289 (1.8)
<b>2D</b>	203 (18.1)	255 (13.3)	289 (1.6)
<b>1A</b>	212 (16.0)	229 (16.2)	274 (4.9)
<b>2A</b>		235 (14.9)	

[a] Absorption maxima were measured in cyclohexane, while molar

Compound **2A** shows a single absorption at 235 nm, which is attributed to a  $\pi$ – $\pi^*$  transition of the dicyanoethenyl moiety. Compound **1A** possesses an additional band at 274 nm. This transition is absent in the spectra of both dicyanomethylenecyclohexane and 1,1'-bicyclohexylidene and was identified previously as an intramolecular charge-transfer (CT) absorption, which involves charge transfer from the ethylenic double bond to the dicyanoethenyl acceptor.<sup>[23]</sup>

The absorption spectrum of the saturated donor model **2D** is similar to that of *N*-phenylpiperidine.<sup>[24]</sup> It consists of three bands positioned at 289, 255 and 203 nm. The 289 nm band is

the HOMO–LUMO transition, that is, it is comparable to the  $^1L_b$  transition in benzene. The absorption at 255 nm has been attributed to an intramolecular CT absorption, which involves an interaction between the benzene and amino moieties.<sup>[25]</sup> The absorption spectrum of **1D** is similar to the spectrum of **2D**. However, in **1D** the anilino-type band near 205 nm overlaps with the  $\pi$ – $\pi^*$  transition of the exocyclic double bond, which is situated at 206 nm in bicyclohexylidene.<sup>[10]</sup> Accordingly, the absorption of **1D** in the 200 nm region is more intense.

The spectra of **1DA** and **2DA** have a strong resemblance to the sum spectra of **1D**, **1A** and **2D**, **2A**, respectively.<sup>[26]</sup> No additional absorption bands are present in the spectra of the donor/acceptor compounds. This indicates that no significant coupling between the *N*-phenyl donor and the ethylenic double bond and/or the dicyanoethylene acceptor occurs in the ground state or Franck–Condon excited state. The molar absorption coefficient of the long-wavelength absorption near 290 nm increases from 2300 for **2DA** to about  $5700\text{ M}^{-1}\text{ cm}^{-1}$  for **1DA**; this is due to the additional absorption of the double-bond/acceptor system in the latter (cf. **1A**). Since in most of the time-resolved experiments discussed below an excitation wavelength of 308 nm was used, both the donor and “acceptor” chromophore will be excited in **1DA**, whereas in **2DA** only the dialkylanilino donor will be excited.

**Steady-state emissive properties:** Upon charge separation in DSA compounds, the fluorescence of the local donor and/or acceptor chromophores is strongly quenched. In addition, DSA compounds generally show emission bands that are absent in the spectra of the separate donor and acceptor moieties.<sup>[17, 23]</sup> In general, the CT character of the emissive state is reflected by a strong dependence of the emission wavelength on solvent polarity.<sup>[27]</sup> The fluorescence spectra of **1DA**, **2DA**, and the model compounds (solvents cyclohexane and benzene) are presented in Figure 2. Salient results are collected in Table 2.

**Donor model compounds:** The emissive properties of **1D** and **2D** are similar to those reported for *N*-phenylpiperidine.<sup>[24]</sup> A comparison of the emission spectra of **1D** and **2D** shows no effect of the exocyclic double bond of the former on either the position or quantum yield of the fluorescence. The nature of the solvent has only a limited influence on the position of the emission maximum, while the fluorescence is somewhat stronger in benzene.

**Acceptor model compounds:** Acceptor model **2A** is non-fluorescent; this has been rationalized by invoking rapid, radiationless relaxation accompanied by a twist around the double bond of the dicyanoethylene chromophore in the excited state.<sup>[28]</sup> Compound **1A** shows a broad CT-type emission at 408 nm in benzene. The charge-separated state is a result of electron transfer from the olefinic double bond to the dicyanoethylene acceptor.<sup>[23]</sup> The CT emission is absent in cyclohexane. In this nonpolar solvent the charge-separated excited state is only little stabilized, so that it lies close to the local acceptor singlet excited state. As a consequence of admixture with this local acceptor state the CT state is subject

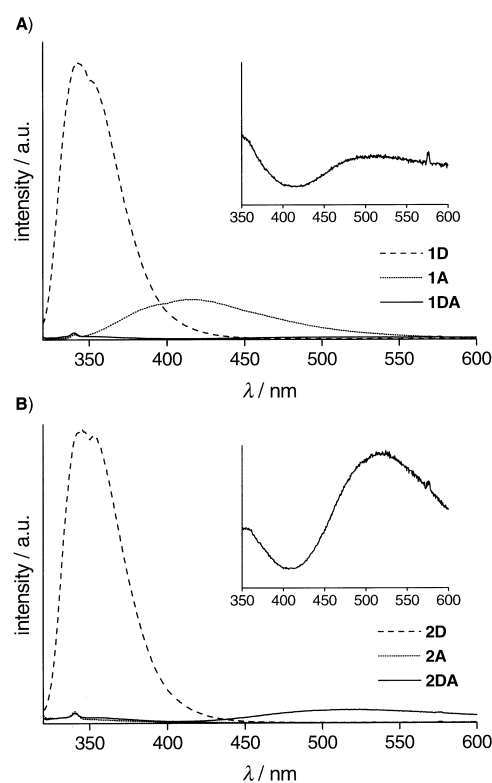


Figure 2. Steady-state emission spectra of A) **1DA**, **1D** and **1A** and B) **2DA**, **2D** and **2A**. All spectra were recorded in benzene. The insets show the magnified spectra of **1DA** and **2DA**.

Table 2. Fluorescence maxima, fluorescence quantum yields  $\Phi_f$ , and fluorescence lifetimes  $\tau$  of DA compounds (**1DA**, **2DA**), donor model compounds (**1D**, **2D**), and acceptor model compound **1A** in cyclohexane and benzene (20 °C).<sup>[a]</sup>

	cyclohexane			benzene		
	$\lambda_{em}$ [nm]	$\Phi_f$	$\tau$ [ns] <sup>[b]</sup>	$\lambda_{em}$ [nm]	$\Phi_f$	$\tau$ [ns] <sup>[b]</sup>
<b>1DA</b>	386, 521	< 0.01, 0.02	< 1, 20	525	0.01	< 1, 2
<b>2DA</b>	336, 494	0.01, 0.03	< 1, 24	515	0.02	< 1, 36
<b>1D</b>	336	0.25	2	343	0.34	2
<b>2D</b>	336	0.25	2	343	0.35	2
<b>1A</b>	— <sup>[c]</sup>	—	—	408	0.03	1

[a] Excitation wavelength used for quantum yield determination: **1D**, **2D** and **1A**: 290 nm; **1DA** and **2DA**: 300 nm. [b] Fluorescence lifetimes determined from (multi)exponential fits at a number of wavelengths. [c] No emission observed.

to rapid radiationless decay and CT fluorescence is not observed in cyclohexane.

**Donor/acceptor compounds:** The intense local donor emission of **1D** is almost completely absent in the emission spectrum of **1DA** in both solvents. The emission of the acceptor/double-bond system, which was seen to be present in the spectrum of **1A** in benzene, is also completely quenched. Instead of these “local” emission bands, a new, weak and broad emission with a maximum at 521 nm (2.38 eV; cyclohexane) or 525 nm (2.36 eV; benzene) is discernible. Similar emission spectra are obtained for **2DA**: local emission from **2D** is effectively quenched and instead a broad emission at 494 nm (2.51 eV; cyclohexane) or 515 nm (2.41 eV; benzene) is found. These results point to the occurrence of charge transfer upon

photoexcitation for **1DA** and **2DA**. Since it is well known that fluorescence resulting from a charge-separated state is strongly dependent on the polarity of the medium, it is surprising that both **1DA** and **2DA** have their emission maxima at approximately the same wavelength in both cyclohexane and benzene. It is expected that a fully stretched CT state will be stabilized in benzene by approximately 0.4 eV with respect to nonpolar cyclohexane.<sup>[29]</sup> This is clearly not the case for **1DA** and **2DA**, which may indicate that in cyclohexane and benzene emission from different excited state conformers is observed (vide infra).

Whether photoinduced charge separation is thermodynamically feasible can be evaluated by application of the Weller equation, which describes the dependence of the driving force for charge separation ( $\Delta G_{CS}$ ) on solvent and donor–acceptor distance.<sup>[30]</sup> Values of  $\Delta G_{CS}$  in cyclohexane ( $\epsilon_s = 2.02$ )<sup>[27]</sup> are  $-0.52$  and  $-0.51$  eV for **1DA** and **2DA**, respectively. In benzene ( $\epsilon_s = 2.28$ )<sup>[27]</sup>  $\Delta G_{CS}$  values are  $-0.66$  for **1DA** and  $-0.63$  eV for **2DA**. These data reveal that photoinduced charge transfer is feasible for the DSA compounds under investigation, even in the nonpolar solvent cyclohexane. They support the experimental observation of charge separation in the form of quenching of local emission and the occurrence of new CT emission bands.

**Time-resolved fluorescence spectroscopy:** Fluorescence lifetimes ( $\tau$ ) were measured at various wavelengths. The lifetimes of the donor and acceptor model compounds (Table 2) are in good agreement with values reported for similar compounds.<sup>[23, 31]</sup> No significant differences are observed between the fluorescence lifetimes of **1D** and **2D** ( $\tau = \text{ca. } 2$  ns). For acceptor model **1A** the CT emission in benzene is also relatively short-lived ( $\tau = \text{ca. } 1$  ns).

A good fit to the emission decay of **1DA** in cyclohexane was obtained by assuming a biexponential decay with a short-lived ( $\tau < 1$  ns) and a long-lived component ( $\tau = 20$  ns). In benzene, however, only two short-lived components are found ( $\tau < 1$  ns, 2 ns). For **2DA** in cyclohexane lifetimes were similar to those of **1DA** ( $\tau < 1$  ns, 24 ns), whereas in benzene a long component of 36 ns is measured for the CT-type emission. For both **1DA** and **2DA** the short-lived components are more prominent at short wavelengths and, hence, they are attributed to residual local donor fluorescence. Thus, in benzene a large difference between the lifetimes of the CT emission is observed (2 and 36 ns, respectively). Apparently, deactivation of the CT excited state in the compound with the bicyclohexylidene bridge (**1DA**) is approximately 20 times faster than in the compound with the bicyclohexyl bridge (**2DA**). In cyclohexane, however, the lifetimes of the CT emission of **1DA** and **2DA** are of similar magnitude (20 and 24 ns, respectively).

The large difference between the fluorescence lifetimes of **1DA** in benzene and cyclohexane again suggests the presence of different conformational states in these solvents. Support for the occurrence of conformational changes upon photoexcitation can be provided by time-dependent changes of fluorescence spectra. Time-resolved fluorescence measurements revealed that only for **2DA** in cyclohexane a wavelength shift of the emission spectrum with time is observed

(Figure 3). The fluorescence maximum initially lies at 440 nm and gradually shifts towards 500 nm. Single-photon-counting experiments showed that the decay of the emission at 440 nm is coupled to the rise of the emission at 500 nm (data not shown). Hence, upon excitation the initially formed excited

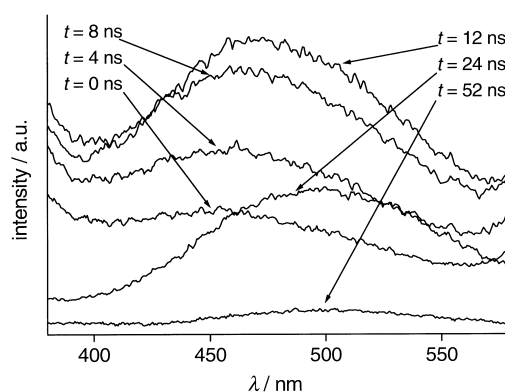


Figure 3. Time-resolved emission spectrum of **2DA** in cyclohexane following flash-photolysis at 308 nm.

species emits at 440 nm (2.82 eV) and converts into a second species that emits at 500 nm (2.48 eV). If it is assumed that the species emitting at 440 nm in cyclohexane is in a stretched conformation, then its energy should be approximately 0.4 eV lower in benzene. This is in good agreement with the steady state emission maximum of **2DA** in benzene (515 nm, 2.41 eV). Thus, the emission bands at 440 nm in cyclohexane and 515 nm in benzene are attributed to a stretched CT species, whereas the conformation of the finally formed species in cyclohexane (emitting near 500 nm) is more compact. Hence, for **2DA** a change in molecular geometry after charge separation is observed, involving folding from an extended conformation to a compact conformation, which as a consequence of the larger Coulomb stabilization emits at a longer wavelength. The fact that in benzene no time dependence of the emission is observed suggests that in this solvent the stretched charge-separated state is stable with respect to folding. A similar behavior has been reported for other types of donor/acceptor compounds bearing saturated six-membered rings as spacers.<sup>[16, 32, 33]</sup>

A stretched conformation is also anticipated for the CT state of **1DA** in benzene on the basis of its structural resemblance to **2DA** and the position of its CT emission band (525 nm, 2.36 eV). Comparison with the position of the CT emission in cyclohexane (521 nm, 2.38 eV) indicates that in the latter solvent a different, probably folded, conformation must be present. However, no time dependence of the emission wavelength was discernible for **1DA** in cyclohexane, even on the picosecond timescale. This can be rationalized in two ways. i) Photoinduced charge separation takes place in an already folded conformation. ii) Folding occurs on a (sub)-picosecond timescale after charge separation in the stretched conformation. Both interpretations are in line with the lower barrier to ring inversion for **1DA** compared with **2DA**, which followed from the NMR data. A possible folded structure of **1DA** is represented in Figure 4.

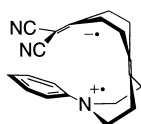


Figure 4. Possible folded structure of **1DA** in the excited state.

**Transient absorption (TA) spectroscopy:** So far, the occurrence of photoinduced charge transfer was assumed on the basis of quenching of local emission and the appearance of new emission bands. More information on the processes

following excitation and the species formed was obtained with transient absorption (TA) spectroscopy with an 8 ns FWHM laser pulse. Transient absorption spectra are shown in Figures 5 and 6, and the absorption maxima and lifetimes are summarized in Table 3.

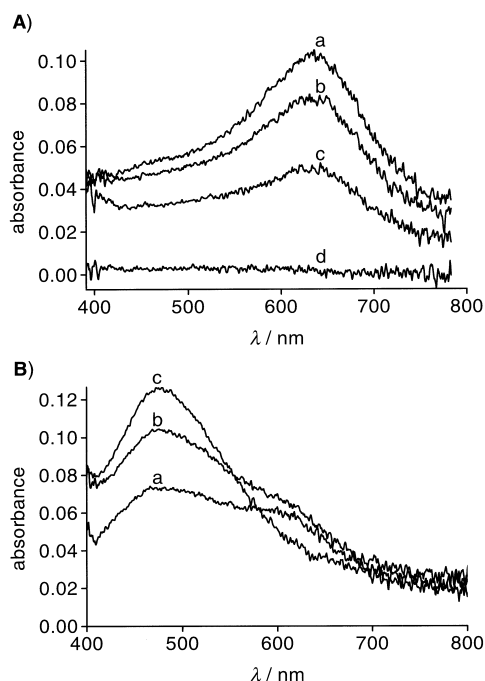


Figure 5. Transient absorption spectra of A) **1D** and B) **2D** in benzene. For A, transients were taken at a) 0, b) 2, c) 4, and d) 20 ns. For B, transients were taken at a) 0, b) 8, and c) 28 ns.

Table 3. Transient absorption maxima and lifetimes  $\tau$  of DA compounds (**1DA**, **2DA**), donor model compounds (**1D**, **2D**), and acceptor model compound (**1A**) in cyclohexane and benzene (20 °C).

	cyclohexane		benzene	
	$\lambda_{\max}$ [nm]	$\tau$ [ns]	$\lambda_{\max}$ [nm]	$\tau$ [ns]
<b>1DA</b>	339, 480	21	339, 460	< 5
<b>2DA</b>	– <sup>[a]</sup>	–	340, 490	35
<b>1D</b>	– <sup>[b]</sup>	–	635	< 5
<b>2D</b>	475	$\gg 20$	475, 625	$\gg 20$
<b>1A</b>	– <sup>[b]</sup>	–	336, 410 <sup>[c]</sup>	< 5

[a] Solubility too low. [b] No absorption observed. [c] 410 nm band due to interference of CT emission (see text).

**Acceptor model compounds:** The TA spectrum of **1A** in benzene displays two bands situated at 336 nm and 410 nm. The 336 nm band is assigned to the dicyanoethylene radical anion.<sup>[34]</sup> The lifetime obtained from TA (< 5 ns) is in agreement with the fluorescence lifetime of 1 ns. The observation of the tetraalkyl olefinic radical cation was hampered

by interference of CT fluorescence near 408 nm, the spectral region in which tetraalkyl olefinic radical cations are known to absorb.<sup>[35]</sup> No radical anion and cation absorption could be observed for **1A** in cyclohexane, which must be a consequence of the very short excited-state lifetime.

**Donor model compounds:** Surprisingly, donor model compounds **1D** and **2D** possess pronouncedly different TA spectra in benzene (Figure 5). For the latter, a prominent absorption is observed at 475 nm (both in benzene and cyclohexane) with a very long lifetime on the timescale used ( $\tau \gg 20$  ns). This absorption band is assigned to a dialkylanilino-type triplet state.<sup>[36]</sup> Hence, one of the relaxation pathways of the  $S_1$  state of **2D** involves intersystem crossing to the triplet state. Furthermore, at short times a distinct band at 625 nm appears, the origin of which is not immediately apparent. The TA spectra of **1D** are remarkably different from those of **2D**. In cyclohexane, no absorption at all is present; this suggests that a triplet state is either not formed or very rapidly depopulated. In benzene, two prominent features can be discerned: the absorption of a dialkylanilino triplet state is completely absent and a broad, short-lived absorption ( $\tau < 5$  ns) is present at 635 nm. Apparently, the presence of an exocyclic double bond in *N*-phenylpiperidine derivatives effectively quenches the dialkylanilino-type triplet state. The absorption bands at 635 nm of **1D** and at 625 nm of **2D** most probably stem from the  $S_1$  state of the dialkylanilino chromophore. This assignment is supported by the agreement between the TA lifetimes at 625/635 nm and the fluorescence lifetimes (Table 2). However, it is not clear why the  $S_1$  state is not observed in cyclohexane.

**Donor/acceptor compounds:** The TA spectra of the donor/acceptor compounds are shown in Figure 6. Because of its low solubility, it was not possible to record a TA spectrum of **2DA** in cyclohexane. In general, the TA spectra reveal the presence of two absorptions that decay concurrently. No long-lived absorptions attributable to dialkylanilino triplet states are observed.

For **1DA**, the band at about 340 nm is attributed to the dicyanoethylene radical anion, whereas the long wavelength absorption in the 460–480 nm region is assigned to the dialkylanilino-type radical cation. The absorption spectrum of the dimethylaniline radical cation is well documented and displays an absorption band at 475 nm.<sup>[37]</sup> In cyclohexane the radical cation absorption is red-shifted by approximately 20 nm relative that observed in benzene and possesses a more narrow and asymmetrical shape. The broadening in benzene is either due to solute–solvent interactions or is caused by an increased interaction between the donor and acceptor chromophores. A similar broadening of the dialkylanilino radical cation absorption due to electronic interaction with another chromophore has been observed for other DSA systems.<sup>[34]</sup> Both the radical cation and radical anion decay in cyclohexane with a lifetime of 21 ns. In benzene, both absorption bands are very short-lived and a lifetime  $\tau < 5$  ns is observed. These lifetimes are in agreement with those derived from fluorescence decay measurements, which corroborates the interpretation of the broad emission bands around about

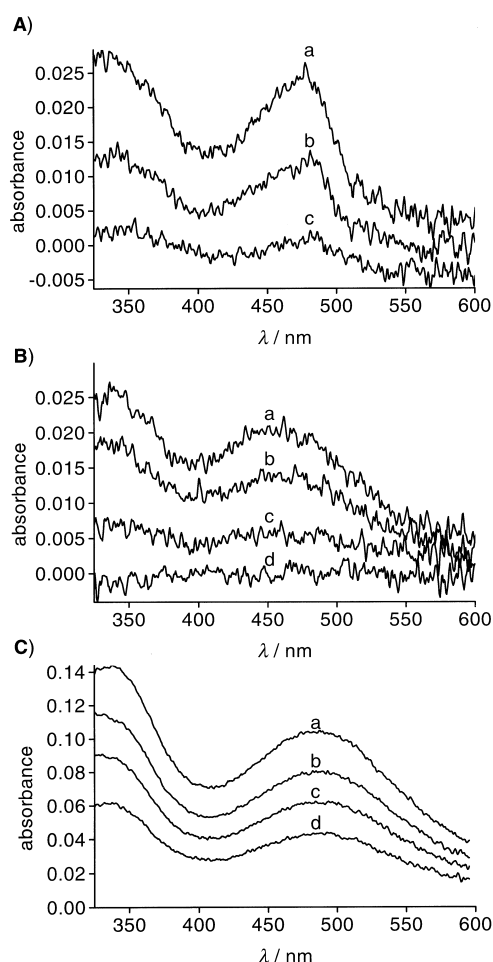


Figure 6. Transient absorption spectra of A) **1DA** in cyclohexane, B) **1DA** in benzene, and C) **2DA** in benzene. For A, transients were taken at a) 0, b) 14, and c) 34 ns. For B, transients were taken at a) 0, b) 4, c) 10, and d) 16 ns. For C, transients were taken at a) 0, b) 10, c) 14, and d) 20 ns.

500 nm as originating from CT states (Table 2). The observation of both dicyanoethylene radical anion and dialkylanilino radical cation absorption bands confirms the formation of a charge-separated state in **1DA** after photoexcitation.

For **2DA** in benzene, absorption bands at 340 and 490 nm are also present; these once again correspond to the dicyanoethylene radical anion and the dialkylanilino radical cation, respectively. When compared with the TA spectrum of **1DA** in benzene, the long-wavelength absorption maximum is red-shifted by approximately 25 nm. This may point to an excited state interaction between the double bond and the dialkylanilino group in **1DA**. For **2DA** both absorptions decay with a lifetime of 35 ns, which is in good agreement with the value of 36 ns obtained from the emission spectra.

**Time-resolved microwave conductivity (TRMC) measurements:** In their excited charge-separated state, the donor/acceptor compounds are expected to possess considerable dipole moments. The TRMC technique is well suited for the determination of these large dipole moments.<sup>[38, 39]</sup> TRMC transients, reflecting the changes in microwave conductivity upon excitation, are shown together with the individual contributions from the excited singlet and triplet state to the

overall fit curve for **1D** and **2D** (benzene) in Figure 7. TRMC traces and fits for donor/acceptor compound **2DA** are depicted in Figure 8. The dipole moments calculated from the best fits to the changes in microwave conductivity (assuming the formation of a single transient dipolar species) and the lifetimes used for the fitting are listed in Table 4. Since the TRMC signal is related to the difference of the excited-state and ground-state dipole moment, use has been made of AM1-calculated ground-state dipole moments to obtain the excited-state dipole moments.

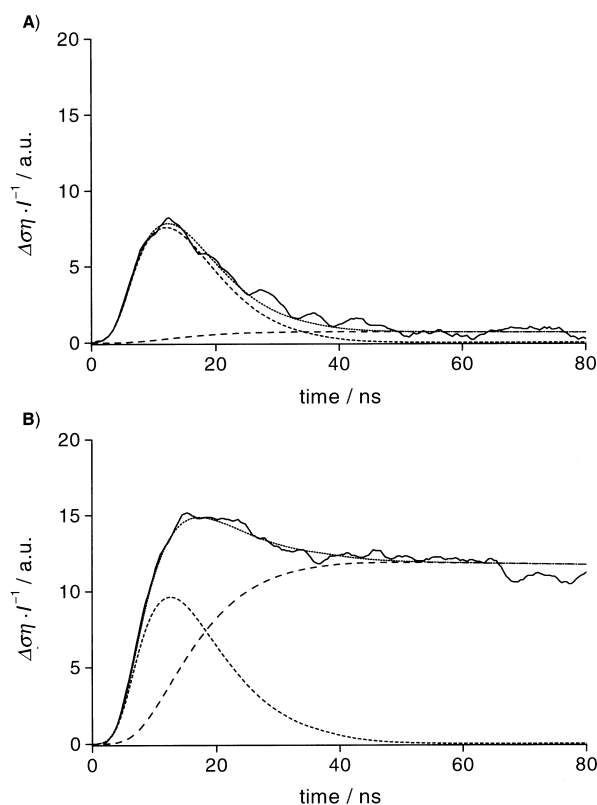


Figure 7. Transient changes in the microwave conductivity (dielectric loss) of benzene solutions of A) **1D** and B) **2D** (solid lines). The dashed lines show the individual contributions from the excited singlet and triplet states to the overall fit curve (dotted line).

Table 4. TRMC data of **1DA**, **2DA**, **1D**, **2D**, and **1A** in cyclohexane and benzene.<sup>[a]</sup>

	cyclohexane			benzene		
	$\tau$ [ns]	$\mu_{\text{sph}}$ [D] <sup>[b]</sup>	$\mu_{\text{cyl}}$ [D] <sup>[b]</sup>	$\tau$ [ns]	$\mu_{\text{sph}}$ [D] <sup>[b]</sup>	$\mu_{\text{cyl}}$ [D] <sup>[b]</sup>
<b>1DA</b>	23	15	23	1.8	17	29
<b>2DA</b>	24	18	29	36	17	29
<b>1D</b>	– <sup>[c]</sup>	–	–	2.4	5	7
<b>2D</b>	– <sup>[c]</sup>	–	–	2.5	6	8
<b>1A</b>	– <sup>[d]</sup>	–	–	1.5	14	19

[a] One unit charge separated by 1 Å gives a dipole moment of 4.8 D. [b] Assuming  $\Phi_{\text{cs}} = 1$  (see text). [c] Not measured. [d] No signal observed in cyclohexane.

**Acceptor model 1A:** The acceptor model **1A** has an appreciable TRMC signal in benzene. An excited-state dipole moment of 19 D is calculated based on a cylindrical geometry; this corresponds to full charge separation over a distance of 3.9 Å. This is close to the spatial separation (ca. 4 Å) between

the olefinic double bond and the double bond of the dicyanoethylene moiety. In cyclohexane no TRMC signal whatsoever is observable for **1A**. This result indicates again that the CT state is rapidly deactivated and corroborates the fluorescence and transient absorption data.

**Donor model compounds:** The TRMC traces of model donors **1D** and **2D** (both in benzene) are markedly different. The transient of **2D** displays an initial component that decays within a few nanoseconds, followed by a component with a lifetime of several microseconds. The fast component is assigned to the excited singlet state of **2D**, while the long-lived component is assigned to the excited triplet state. Similar results have been found for *N,N*-dimethylaniline.<sup>[40]</sup> The TRMC trace of **1D** mainly consists of a short-lived signal, attributed to the excited singlet state, with only a minor contribution of a long-lived triplet state. These observations corroborate the results obtained from the TA experiments, in which a dialkylanilino-type triplet absorption was found for **2D**, whereas no evidence for triplet formation was obtained for **1D**. Singlet excited-state dipole moments of 7.3 D and 8.1 D are calculated for **1D** and **2D**, respectively. These dipole moments are somewhat larger than that of *N,N*-dimethylaniline (5.0 D),<sup>[40]</sup> reflecting a higher degree of charge separation in the excited singlet state.

**Donor/acceptor compounds:** As an illustration, TRMC transients for donor/acceptor compound **2DA** in cyclohexane and benzene are shown in Figure 8. In both solvents, a large

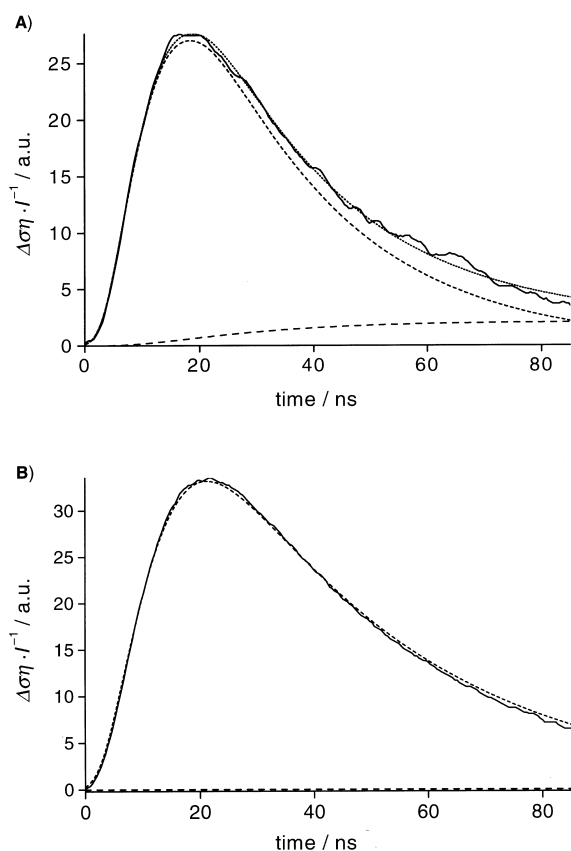


Figure 8. Transient changes in the microwave conductivity (dielectric loss) of **2DA** in A) cyclohexane and B) benzene (solid lines). The dashed lines show the individual contributions from the excited singlet and triplet states to the overall fit curve (dotted line).

signal with a relatively long lifetime, assigned to the singlet excited state, is found. This lifetime is significantly longer in benzene (36 ns) than in cyclohexane (25 ns). Furthermore, the contribution of the triplet state to the TRMC signal is small in cyclohexane, and virtually absent in benzene. The lifetimes of the excited states used for the fitting of the TRMC traces (for both **1DA** and **2DA**) are in good agreement with those obtained from both time-resolved fluorescence and TA spectroscopy.

The absolute values of the excited-state dipole moments of **1DA** and **2DA** can be calculated on the basis of either a spherical geometry or a cylindrical geometry of the charge-separated species.<sup>[38, 39]</sup> For the folded conformation in cyclohexane, the former geometry is a reasonable approximation, whereas the latter is suitable for the calculation of the dipole moment of the stretched conformer as found in benzene. Thus, in cyclohexane a dipole moment of 15 D is obtained for **1DA** and 18 D for **2DA**. From these values it appears that the donor and acceptor are somewhat closer together in **1DA**; this may find its origin in different conformations in the excited states of the two compounds.

A value of 29 D is obtained for the excited-state dipole moment of both **1DA** and **2DA** in benzene. Note that these dipole moments are calculated under the assumption of a quantum yield of unity for the formation of a charge-separated species. The excited-state dipole moments of **1DA** and **2DA** in benzene are somewhat smaller than the expected values of 37 and 38 D for full charge separation over a donor–acceptor distance of 7.7 and 7.9 Å,<sup>[30]</sup> respectively. Since the TA data revealed the formation of the both the dicyanoethylene radical anion and the anilino radical cation, full charge separation nevertheless must occur. It could be that the quantum yield for charge separation is less than unity, which might explain why the TRMC excited-state dipole moments do not reflect full charge separation. However, the virtually complete quenching of the local donor and acceptor emission in the fluorescence spectra of **1DA** and **2DA** strongly suggests that formation of the charge-separated state [ $D^+SA^-$ ]\* is quantitative. The most likely explanation for the small excited-state dipole moments left is that the geometry of **1DA** and **2DA** in the CT state in benzene is not a fully stretched conformation, such as has been assumed until now. The dipole moment of 29 D corresponds to full charge separation over approximately 6 Å. This suggests that **1DA** and **2DA** are in a bent or partially folded conformation. For instance, in Figure 9 a structure of **1DA** is depicted in which only the piperidine ring adopts a boat conformation and where the donor–acceptor distance is about 6 Å. Although it is not certain that this is the correct structure for the CT state of **1DA** and **2DA** in benzene, this shows that conformations are possible in which the donor–acceptor distance is approximately 6 Å. We note that the actual values of the excited state dipole moments are affected when the geometry of the compounds is not a real cylinder, which may lead to some error in the derived dipole moments.

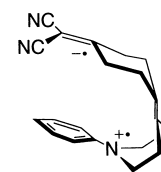


Figure 9. Partly folded structure of **1DA** in the excited state.



## Conclusion

As judged from the similar absorption spectra of **1D** and **2D**, a significant ground-state interaction of the exocyclic double bond with the anilino donor does not seem to be present. In contrast, the absorption spectrum of acceptor model compound **1A** clearly shows that the double bond interacts with the dicyanoethylene acceptor in the ground state, giving rise to a charge-separated state upon excitation. Unfortunately, owing to the ultrafast nature of the charge-separation process in **1DA** and **2DA**, it was not possible to obtain any information on the effect of the presence of the double bond on this process. Nevertheless, the presence of the exocyclic double bond in the bicyclohexylidene-type bridge system is manifest in essentially three ways. Firstly, the double bond renders the bridge much more flexible, facilitating the occurrence of conformational changes in the excited state. Thus, in cyclohexane folding takes place subsequent to charge separation for **2DA** (on a nanosecond timescale), whereas for **1DA** folding takes place either prior to charge separation, or on a subpicosecond timescale after charge separation in the bent or partially folded geometry. Secondly, as shown by both the TA and TRMC data, the presence of the exocyclic double bond results in the triplet state of the local anilino donor not being observed. Thirdly, as indicated by the fluorescence and TRMC lifetimes of **1DA** and **2DA** in benzene, the decay of the extended CT species is about 20 times faster in presence of the double bond. A similar effect, albeit less pronounced, has been reported for compounds differing from **1DA** and **2DA** in the donor and acceptor chromophores.<sup>[33]</sup>

The fact that an anilino triplet state is not observed in the presence of the exocyclic double bond (compound **1D**) can be understood by considering the triplet state energies of the anilino and tetraalkylethylene chromophores. From the phosphorescence spectrum of *N,N*-dimethylaniline,<sup>[41]</sup> the energy of the triplet state  $T_1$  of the anilino chromophore is estimated to be 3.3 eV. The triplet energy of the double bond in the present compounds is not exactly known, but it is expected to be similar to or slightly lower than the triplet energy of tetramethylethene, which is also about 3.3 eV.<sup>[42]</sup> Therefore, we expect that once the  $T_1$  of the anilino chromophore is populated, triplet–triplet energy transfer to the ethylene triplet state occurs which prevents the anilino triplet from being detected. Subsequently, the ethylene triplet state is rapidly deactivated by radiationless decay.<sup>[41]</sup>

The role of the olefinic double bond in the faster decay of the CT state of **1DA** relative to **2DA** in benzene may be twofold. Firstly, it is likely that it increases the coupling between the CT state and the locally excited or ground state, thereby favoring charge recombination. Secondly, as shown above, through its triplet state the double bond also generates an additional recombination pathway. The importance of this decay channel can, however, only be small, since in cyclohexane the folded CT-state lifetime of **1DA** is only slightly shorter than the folded CT-state lifetime of **2DA**. Note that for **1DA** the compact CT state in cyclohexane has about the same energy as the stretched conformation in benzene, so that the energetic distance to the ethylenic triplet state is the same for both conformations. It is therefore likely that the effect of

the presence of the double bond on the recombination kinetics predominantly stems from the increased coupling between the stretched CT state and the locally excited or ground state.

In summary, we have shown that photoinduced electron transfer occurs in donor/acceptor-substituted bicyclohexylidenes and bicyclohexyls, and that the presence of the exocyclic double bond has a strong influence on the photo-physical properties of these compounds. In this context, it is interesting that also in longer oligo(cyclohexylidene) DSA compounds the local emission of the dialkylanilino chromophore is partly quenched; this indicates that even over a distance of 16.1 Å (three intervening cyclohexylidene rings) through-bond interaction between the donor and acceptor chromophore must exist.<sup>[9b]</sup>

## Experimental Section

**General:** All reactions were carried out under a dry nitrogen atmosphere unless stated otherwise. Commercially available reagents were used without purification. THF was distilled from sodium/benzophenone prior to use. Acetonitrile was stored over 3 Å molecular sieves. For column chromatography silica (Merck kieselgel 60, 230–400 mesh ASTM) was used. Melting points were determined by using a Mettler FP5/FP51 photoelectric melting point apparatus and are uncorrected. NMR spectra were recorded on a Bruker AC 300 spectrometer, operating at 300.13 MHz for <sup>1</sup>H NMR and 75.47 MHz for <sup>13</sup>C NMR spectroscopy. Chemical shifts are given relative to external TMS. Samples were dissolved in deuterated chloroform unless stated otherwise. Infrared spectra of solids were recorded on a Mattson Galaxy Series FTIR 5000 spectrophotometer with a diffuse reflectance accessory; samples were diluted with optically pure KBr. Elemental analyses were carried out by H. Kolbe Mikroanalytisches Laboratorium, Mülheim a.d. Ruhr (Germany). UV spectra were measured with a Cary 1 UV/Vis spectrophotometer in spectrophotometric grade solvents (Janssen/Acros). Fluorescence spectra were obtained on a Spex Fluorolog instrument.<sup>[43]</sup> Fluorescence quantum yields were determined relative to naphthalene ( $\Phi_f = 0.23$ )<sup>[44]</sup> (compounds **1D** and **2D**) or 9,10-diphenylanthracene ( $\Phi_f = 0.90$ )<sup>[44]</sup> (compounds **1A**, **1DA**, **2DA**). Samples were diluted to  $A_{1\text{cm}} < 0.1$  at the excitation wavelength used and deoxygenated by purging with argon for 15 minutes. Redox potentials were determined by using cyclic voltammetry conducted with a Heka PG 287 potentiostat/galvanostat in acetonitrile (Janssen p.a. grade, freshly distilled from calcium hydride) containing 0.1 M tetrabutylammonium hexafluorophosphate (Fluka, electrochemical grade) as supporting electrolyte. The scanning rate was 0.1 V s<sup>-1</sup>. Oxidation and reduction potentials were determined relative to Ag/AgNO<sub>3</sub> (0.1 M in acetonitrile) and were referenced to SCE by regularly measuring the oxidation potential of the FeCp/FeCp<sup>+</sup> couple ( $E_{1/2}$  vs. SCE = 0.31 V).<sup>[44]</sup> Both the oxidation process of the *N*-phenylpiperidino donors and the reduction process of the dicyanoethylene acceptor were irreversible. The half-wave potentials were obtained by correction of the peak maxima with +30 mV for the cathodic wave and –30 mV for the anodic wave.

**Time-resolved fluorescence measurements:** Fluorescence lifetimes were determined at single wavelengths by using a Lumonics EX700 pulsemaster XeCl excimer laser (308 nm, 8 ns FWHM) as excitation source. The emitted light was passed through a Carl Zeiss M4QII monochromator and detected using an RCA 1P28 photomultiplier. The signal of the detector was fed into a TDS684A digital oscilloscope, which was triggered by a photodiode that detects the laser light pulse. Data were analyzed by a program based on iterative convolution which allows the calculation of fluorescence lifetimes for mono-, bi- and tri-exponential decay functions. Samples ( $A_{1\text{cm}}(308\text{ nm}) < 0.1$ ) were degassed by purging with argon for 15 min. The equipment used for picosecond single photon-counting measurements has been fully described elsewhere.<sup>[46]</sup> Time-resolved fluorescence spectra (Figure 3) were obtained by using the experimental set-up described below for transient absorption spectroscopy, but without the xenon lamp as probe light.

**Transient absorption spectroscopy:** TA spectra were obtained by using a Lumonics EX700 XeCl excimer laser (308 nm) as the excitation source and a 450 W high-pressure Xe-arc, pulsed with a Müller Elektronik MSP05 pulser to enhance its brightness during the observation time gate of the detector, in right angle geometry as probe light. The probe light, after passing through the sample cell, was collected by an optical fibre and fed into a Jarrel-Ash monospec 27 model 1234 spectrograph in which the light was dispersed by a grating (150 grooves mm<sup>-1</sup>) onto an MCP-intensified diode array detector (EG&G 1421G, 25 mm, 1024 diodes). With this set-up a spectral range of about 600 nm was covered with a bandwidth of 7 nm (250 µm slit). The detector was gated at 5 ns by an EG&G 1302 pulse generator and the start of the time window was delayed in 2 or 5 ns increments relative to the laser pulse to obtain subsequent spectra across the total decay time of the transients studied. The timing of the laser, the probe light, and the optical multichannel analyser (OMA) gate pulse was controlled by an EG&G OMA III Model 1460 console with a 1303 pulse generator and a digital delay generator (EG&G 9650). Spectra were averaged over ≤20 pulses for each delay to improve the signal to noise ratio. Samples were prepared in spectrophotometric grade cyclohexane and benzene in a concentration  $0.8 < A_{1\text{cm}}(308 \text{ nm}) < 1.5$  and were degassed by several freeze-pump-thaw cycles.

**Time-resolved microwave conductivity measurements:** In a TRMC experiment, a solution of the compound under investigation in a non-dipolar solvent, contained in a microwave cavity, was photoexcited by a 7 ns laser flash from a XeCl excimer laser. The formation of a dipolar excited state lead to an increase in the high-frequency dielectric loss of the solution. This increase was monitored by time-resolved measurement of the change in microwave conductivity  $\Delta\sigma$  which is related to the difference in excited-state and ground-state dipole moment. It was necessary for the calculation of the excited state dipole moment from the TRMC transients to describe the geometry of the charge-separated species properly. Methods are available for spherical, cylindrical, and disklike molecular geometries. The technique is described in detail elsewhere.<sup>[38, 39]</sup> Samples with  $A_{1\text{cm}}(308 \text{ nm}) > 0.3$  and preferably  $A_{1\text{cm}}(308 \text{ nm}) = 1$  were prepared in UV spectroscopic grade cyclohexane and benzene and were deaerated by purging with CO<sub>2</sub> for 15 min. The solutions contained in a microwave cavity were flash-photolysed by using a single 7 ns FWHM pulse (308 nm) of a Lumonics HyperEX 400 excimer laser. Any transient change occurring in the microwave conductivity (dielectric loss) of the solution was monitored as a change in the microwave power reflected by the cavity by using a Tektronix 7912 transient digitizer.

#### Synthesis of donor/acceptor compounds

**9-(1-Phenyl-4-hydroxy-piperidin-4-yl)-3,3-dimethyl-1,5-dioxaspiro[5.5]undecane-9-carboxylic acid (6):** A two-necked flask was filled with THF (150 mL) and diisopropylamine (19.05 g, 189 mmol). Butyllithium in *n*-hexane (131 mL of a 1.46 M solution, 191 mmol) was added to this solution at -40 °C, and after stirring for 30 min 3,3-dimethyl-1,5-dioxaspiro[5.5]undecane-9-carboxylic acid<sup>[9]</sup> (**5**; 21.35 g, 93.6 mmol) in THF (25 mL) was added at once at -40 °C. The reaction mixture was then stirred at 50 °C for two hours and re-cooled to -40 °C. *N*-Phenyl-4-piperidone<sup>[17]</sup> (**4**; 16.84 g, 96.2 mmol) in THF (25 mL) was then added at once, and the reaction mixture was stirred at 50 °C for another 2 h. After cooling to room temperature the mixture was poured on ice (750 g) and diluted with diethyl ether (500 mL). The layers were separated and the organic layer was extracted with water (2 × 150 mL). The combined water layers were washed with diethyl ether (2 × 100 mL) and subsequently acidified to pH 1 using 3 M hydrochloric acid. The resulting white precipitate was filtered off, washed with water, and dried in vacuo over potassium hydroxide, yielding a white solid (13.70 g, 34.0 mmol, 36 %). M.p. 222 °C (decomp); <sup>1</sup>H NMR ([D<sub>6</sub>]DMSO):  $\delta = 7.81$  (m, 2H), 7.52 (m, 2H), 7.47 (m, 1H), 3.68 (m, 2H), 3.38 (m, 6H), 2.40 (m, 2H), 2.19 (m, 2H), 1.92 (m, 4H), 1.60 (m, 2H), 1.21 (m, 2H), 0.87 (s, 6H); IR (KBr):  $\tilde{\nu} = 3500\text{--}3000, 2976, 2957, 2949, 2903, 2868, 2900\text{--}2300, 1732, 1694, 1494, 1469, 1448, 1105, 756, 691 \text{ cm}^{-1}$ .

**9-(1-Phenylpiperidin-4-ylidene)-3,3-dimethyl-1,5-dioxaspiro[5.5]undecane (7):** *N,N*-Dimethylformamide dineopentyl acetal (15.65 g, 67.6 mmol) was added to a suspension of  $\beta$ -hydroxy acid **6** (13.45 g, 33.4 mmol) in acetonitrile (375 mL) and after stirring for 1 h at room temperature the reaction mixture was heated to reflux overnight. The resulting yellow solution was cooled to -20 °C, and the resulting precipitate was filtered off, washed with cold acetonitrile, and dried to yield a white powder (8.12 g,

23.8 mmol, 71 %). M.p. 166–167 °C; <sup>1</sup>H NMR:  $\delta = 7.25$  (m, 2H), 6.92 (d,  $J = 7.9$  Hz, 2H), 6.81 (t,  $J = 7.3$  Hz, 1H), 3.54 (s, 4H), 3.21 (t,  $J = 5.7$  Hz, 4H), 2.46 (t,  $J = 5.7$  Hz, 4H), 2.28 (m, 4H), 1.83 (m, 4H), 0.99 (s, 6H); <sup>13</sup>C NMR:  $\delta = 151.38, 129.36, 129.06, 126.07, 118.90, 115.98, 97.68, 70.12, 50.60, 33.46, 30.25, 29.11, 25.05, 22.76$ ; IR (KBr):  $\tilde{\nu} = 3094, 3069, 3036, 3017, 2974, 2967, 2955, 2940, 2920, 2893, 2866, 2847, 2828, 1597, 1576, 1479, 1462, 1448, 1431, 1117, 752, 687 \text{ cm}^{-1}$ .

**4-(1-Phenylpiperidin-4-ylidene)cyclohexanone (8):** Acetal **7** (8.12 g, 23.8 mmol) was dissolved in THF (70 mL), and 5 % hydrochloric acid (70 mL) was added. The mixture was heated to reflux for 4 h. After cooling to room temperature, THF was removed at reduced pressure and the resulting suspension was extracted with chloroform (2 × 75 mL). After washing the combined organic extracts with saturated NaHCO<sub>3</sub> solution and water, respectively, drying (MgSO<sub>4</sub>), and evaporation of the solvent, an off-white solid was obtained (5.61 g, 22.0 mmol, 92 %). M.p. 58–60 °C; <sup>1</sup>H NMR:  $\delta = 7.27$  (m, 2H), 6.94 (d,  $J = 7.9$  Hz, 2H), 6.84 (t,  $J = 7.3$  Hz, 1H), 3.26 (t,  $J = 5.8$  Hz, 4H), 2.60 (t,  $J = 6.7$  Hz, 4H), 2.50 (t,  $J = 5.7$  Hz, 4H), 2.43 (t,  $J = 6.8$  Hz, 4H); <sup>13</sup>C NMR:  $\delta = 212.32, 151.18, 129.13, 129.13, 125.54, 119.10, 116.00, 50.22, 40.55, 29.22, 26.54$ ; IR (KBr):  $\tilde{\nu} = 3090, 3055, 3040, 2963, 2915, 2897, 2849, 2836, 2818, 2805, 1721, 1599, 1494, 1442, 1427, 1415, 762, 694 \text{ cm}^{-1}$ .

**4-(1-Phenylpiperidin-4-ylidene)cyclohexylidenepropanedinitrile (1DA):** A mixture of ketone **8** (2.35 g, 9.22 mmol), malononitrile (1.05 g, 15.9 mmol), ammonium acetate (0.81 g), and acetic acid (2.0 mL) in benzene (100 mL) was heated to reflux for 2 h in a Dean–Stark apparatus. Upon cooling a greenish precipitate formed, which was filtered off and washed with benzene. Yield: 1.47 g (4.85 mmol, 53 %) of a greenish solid. M.p. 170 °C (decomp); <sup>1</sup>H NMR:  $\delta = 7.25$  (m, 2H), 6.90 (d,  $J = 8.0$  Hz, 2H), 6.85 (t,  $J = 7.2$  Hz, 1H), 3.20 (t,  $J = 5.4$  Hz, 4H), 2.78 (t,  $J = 6.0$  Hz, 4H), 2.45 (m, 8H); <sup>13</sup>C NMR:  $\delta = 184.25, 150.94, 130.32, 129.16, 124.54, 119.30, 116.07, 111.60, 83.26, 50.25, 34.42, 29.22, 28.13$ ; IR (KBr):  $\tilde{\nu} = 3092, 3034, 2992, 2965, 2897, 2839, 2822, 2230, 1597, 1504, 1464, 1437, 754, 687 \text{ cm}^{-1}$ ; elemental analysis calcd (%) for C<sub>20</sub>H<sub>21</sub>N<sub>3</sub> (303.41): C 79.16, H 6.98, N 13.86; found C 79.20, H 6.90, N 13.89.

**9-(1-Phenylpiperidin-4-yl)-3,3-dimethyl-1,5-dioxaspiro[5.5]undecane (9):** Acetal **7** (2.70 g, 7.92 mmol) in THF (450 mL) was stirred overnight under an atmosphere of hydrogen (1 atm) in the presence of 10 % Pd/C as a catalyst. Filtration over Celite and evaporation of the solvent gave a white solid in quantitative yield. M.p. 137–139 °C; <sup>1</sup>H NMR:  $\delta = 7.26$  (m, 2H), 6.92 (d,  $J = 8.3$  Hz, 2H), 6.82 (t,  $J = 7.3$  Hz, 1H), 3.70 (brd,  $J = 11.8$  Hz, 2H), 3.53 (s, 2H), 3.48 (s, 2H), 2.63 (brt,  $J = 11.3$  Hz, 2H), 2.38 (m, 2H), 1.78 (brd,  $J = 12.4$  Hz, 2H), 1.63 (m, 2H), 1.50–1.10 (m, 8H), 0.94 (s, 6H); <sup>13</sup>C NMR:  $\delta = 151.92, 128.99, 119.23, 116.48, 97.71, 70.07, 69.86, 50.37, 41.90, 40.65, 32.15, 30.20, 29.60, 25.73, 22.74$ ; IR (KBr):  $\tilde{\nu} = 3096, 3069, 3040, 3025, 2951, 2904, 2864, 2830, 2812, 1599, 1460, 1440, 1111, 1099, 752, 687 \text{ cm}^{-1}$ .

**4-(1-Phenylpiperidin-4-yl)cyclohexanone (10):** Hydrolysis of acetal **9** (2.21 g, 6.44 mmol) as described for **8** quantitatively afforded a white solid. M.p. 137 °C; <sup>1</sup>H NMR:  $\delta = 7.25$  (m, 2H), 6.95 (d,  $J = 7.9$  Hz, 2H), 6.82 (t,  $J = 7.3$  Hz, 1H), 3.70 (brd,  $J = 13.0$  Hz, 2H), 2.65 (brt,  $J = 12.1$  Hz, 2H), 2.35 (m, 4H), 2.08 (m, 2H), 1.70–1.00 (m, 8H); <sup>13</sup>C NMR:  $\delta = 212.12, 151.75, 129.06, 119.47, 116.67, 50.22, 40.98, 40.93, 40.07, 29.85, 29.61$ ; IR (KBr):  $\tilde{\nu} = 3088, 3067, 3034, 3019, 2951, 2938, 2911, 2880, 2863, 2849, 2824, 2809, 1723, 1599, 1502, 1462, 1447, 1431, 1416, 761, 692 \text{ cm}^{-1}$ .

**4-(1-Phenylpiperidin-4-yl)cyclohexylidenepropanedinitrile (2DA):** A mixture of ketone **10** (1.52 g, 5.91 mmol), malononitrile (0.51 g, 7.73 mmol), ammonium acetate (0.44 g), and acetic acid (1.0 mL) in benzene (150 mL) was heated to reflux for 2 h in a Dean–Stark apparatus. Upon cooling, a precipitate formed that was filtered, washed with benzene, and dried to give a greenish solid, which was purified by column chromatography (silica; eluent chloroform). Yield 1.10 g (3.61 mmol, 61 %) of a greenish solid. M.p. 211 °C (decomp); <sup>1</sup>H NMR:  $\delta = 7.23$  (m, 2H), 6.92 (d,  $J = 8.1$  Hz, 2H), 6.82 (t,  $J = 7.2$  Hz, 1H), 3.72 (dt,  $J = 12.4, 2.3$  Hz, 2H), 3.09 (brd,  $J = 13.5$  Hz, 2H), 2.62 (td,  $J = 12.1, 2.3$  Hz, 2H), 2.33 (td,  $J = 13.5, 5.1$  Hz, 2H), 2.17 (brd,  $J = 13.1$  Hz, 2H), 1.80 (brd,  $J = 13.1$  Hz, 2H), 1.60–1.20 (m, 6H); <sup>13</sup>C NMR:  $\delta = 184.51, 151.65, 129.09, 119.60, 116.61, 111.64, 82.69, 50.21, 41.23, 40.07, 34.19, 30.86, 29.49$ ; IR (KBr):  $\tilde{\nu} = 3094, 3074, 3046, 3030, 3015, 2990, 2969, 2942, 2909, 2866, 2843, 2826, 2226, 1595, 1503, 1460, 1442, 1429, 1418, 760, 688 \text{ cm}^{-1}$ ; elemental analysis calcd (%) for C<sub>20</sub>H<sub>23</sub>N<sub>3</sub> (305.43): C 78.64, H 7.60, N 13.76; found C 78.49, H 7.53, N 13.65.

## Synthesis of model donor compounds

**1-(1-Phenyl-4-hydroxy-piperidin-4-yl)cyclohexanecarboxylic acid (11):** This compound was synthesized as described for  $\beta$ -hydroxy acid **6** from cyclohexane carboxylic acid (5.25 g, 41.0 mmol) and *N*-phenyl-4-piperidone **4** (7.02 g, 40.1 mmol) by using butyllithium in *n*-hexane (1.46 M, 58 mL, 84.7 mmol) and diisopropylamine (8.24 g, 81.6 mmol) in THF (150 mL). The crude reaction mixture was poured on ice (150 g) and diluted with diethyl ether (200 mL). The water layer was separated and the organic layer was extracted with water (2  $\times$  50 mL). The combined water layers were washed with diethylether (2  $\times$  25 mL) and subsequently acidified to pH 6 by using 3 M hydrochloric acid. The resulting white precipitate was filtered off, washed with water, and dried in vacuo over potassium hydroxide. Yield 5.55 g (18.3 mmol, 45%). M.p. 225 °C (decomp); IR (KBr):  $\tilde{\nu}$  = 3400–3200, 3067, 3056, 2982, 2968, 2932, 2854, 1687, 1654, 1494, 1462, 1450, 1437, 1131, 761, 700 cm<sup>-1</sup>.

**1-Phenyl-4-cyclohexylidenepiperidine (1D):** This compound was synthesized from **11** (5.55 g, 18.0 mmol) and *N,N*-dimethylformamide dioneopentylacetal (9.05 g, 39.1 mmol) in acetonitrile (250 mL) as described for **7**. The crude reaction mixture was concentrated by evaporation of the solvent to ca. 70 mL and stored at –20 °C. A white solid precipitated, was filtered, washed with cold acetonitrile, and dried to yield 2.58 g of **1D**. The filtrate was diluted with chloroform (150 mL), washed with a saturated NaHCO<sub>3</sub> solution (100 mL) and water (2  $\times$  100 mL), and after separation of the layers, drying of the organic layer (MgSO<sub>4</sub>), and evaporation to dryness a white solid was isolated. Recrystallization of the solid from methanol afforded another 0.45 g (2.0 mmol) of **1D**. Total yield 3.03 g (12.6 mmol, 70%). M.p. 81 °C; <sup>1</sup>H NMR:  $\delta$  = 7.27 (m, 2H), 6.94 (d, *J* = 7.9 Hz, 2H), 6.82 (t, *J* = 7.3 Hz, 1H), 3.22 (t, *J* = 5.8 Hz, 4H), 2.46 (t, *J* = 5.8 Hz, 4H), 2.22 (m, 4H), 1.56 (m, 6H); <sup>13</sup>C NMR:  $\delta$  = 151.54, 131.70, 129.10, 124.77, 118.84, 115.97, 50.73, 30.21, 29.02, 28.60, 27.20; IR (KBr):  $\tilde{\nu}$  = 3096, 3071, 3040, 2972, 2955, 2924, 2887, 2852, 2814, 1599, 1505, 1458, 1447, 1425, 745, 682 cm<sup>-1</sup>; elemental analysis calcd (%) for C<sub>17</sub>H<sub>23</sub>N (241.38): C 84.58, H 9.61, N 5.81; found C 84.30, H 9.59, N 5.77.

**1-Phenyl-4-cyclohexylpiperidine (2D):** 1-Phenyl-4-cyclohexylidenepiperidine **1D** (1.55 g, 6.43 mmol) in THF (250 mL) was stirred overnight under an atmosphere of hydrogen (1 atm) using 10% Pd/C as a catalyst (500 mg). The reaction mixture was filtered over Celite and evaporated to dryness. The crude solid was recrystallized from methanol, yielding 1.00 g (4.12 mmol, 64%) of a white solid. M.p. 97–100 °C; <sup>1</sup>H NMR:  $\delta$  = 7.23 (m, 2H), 6.95 (d, *J* = 8.0 Hz, 2H), 6.83 (t, *J* = 7.25 Hz, 1H), 3.69 (brd, *J* = 12.2 Hz, 2H), 2.65 (td, *J* = 12.2, 2.2 Hz, 2H), 1.75 (m, 7H), 1.40 (m, 2H), 1.20 (m, 5H), 0.97 (m, 2H); <sup>13</sup>C NMR:  $\delta$  = 152.01, 129.00, 119.18, 116.49, 50.48, 42.60, 41.46, 30.19, 29.40, 26.78, 26.68; IR (KBr):  $\tilde{\nu}$  = 3092, 3069, 3032, 3019, 2920, 2870, 2849, 1599, 1503, 1460, 1447, 752, 687 cm<sup>-1</sup>; elemental analysis calcd (%) for C<sub>17</sub>H<sub>25</sub>N (243.40): C 83.88, H 10.36, N 5.76; found C 83.74, H 10.30, N 5.77.

## Synthesis of model acceptor compounds

**1,1'-Bicyclohexyliden-4-ylidenepropanedinitrile (1A):** A mixture of 1,1'-bicyclohexyliden-4-one<sup>[9]</sup> (1.0 g, 5.62 mmol), malononitrile (0.38 g, 5.76 mmol), ammonium acetate (0.46 g), and acetic acid (1.0 mL) was refluxed in benzene (50 mL) for 1.5 h. The crude reaction mixture was washed with water (20 mL), saturated NaHCO<sub>3</sub> solution (20 mL), and again with water (20 mL), dried (MgSO<sub>4</sub>), and evaporated to dryness. The crude solid was recrystallized from ethyl acetate (20 mL) to yield light yellow needles (1.10 g, 4.87 mmol, 87%). M.p. 154–155 °C; <sup>1</sup>H NMR:  $\delta$  = 2.72 (t, *J* = 6.5 Hz, 4H), 2.47 (t, *J* = 6.5 Hz, 4H), 2.19 (m, 4H), 1.54 (m, 6H); <sup>13</sup>C NMR:  $\delta$  = 185.00, 134.93, 122.21, 111.67, 82.89, 34.74, 30.38, 28.25, 28.20, 26.77; IR (KBr):  $\tilde{\nu}$  = 2967, 2927, 2854, 2828, 2229, 1584, 1449, 1431, 999 cm<sup>-1</sup>.

**1,1'-Bicyclohexyl-4-ylidenepropanedinitrile (2A):** This compound was obtained as described for **1A** from 1,1'-bicyclohexyl-4-one (253 mg, 1.41 mmol),<sup>[18]</sup> malononitrile (103 mg, 1.56 mmol), acetic acid (0.2 mL), and ammonium acetate (154 mg) in benzene (50 mL). The crude material was recrystallized from methanol to yield white needles (284 mg, 1.25 mmol, 89%). M.p. 53–55 °C; <sup>1</sup>H NMR:  $\delta$  = 3.01 (brd, *J* = 13.0 Hz, 2H), 2.29 (td, *J* = 12.9, 5.1 Hz, 2H), 2.04 (m, 2H), 1.67 (m, 6H), 1.40–1.00 (m, 8H); <sup>13</sup>C NMR:  $\delta$  = 185.28, 111.71, 82.75, 41.88, 41.83, 34.38, 30.88, 30.22, 26.52, 26.50; IR (KBr):  $\tilde{\nu}$  = 2926, 2853, 2662, 2230, 1595, 1448 cm<sup>-1</sup>.

- [1] R. A. Marcus, N. Sutin, *Biochim. Biophys. Acta* **1985**, *811*, 265.
- [2] M. R. Wasielewski, *Chem. Rev.* **1992**, *92*, 435.
- [3] W. Schuddeboom, B. Krijnen, J. W. Verhoeven, E. G. J. Staring, G. L. J. A. Rikken, H. Oevering, *Chem. Phys. Lett.* **1991**, *179*, 73.
- [4] For a review see: *New J. Chem.* **1991**, *15*, special issue on molecular electronics.
- [5] M. N. Paddon-Row, *Acc. Chem. Res.* **1994**, *27*, 18, and references cited therein.
- [6] R. Hoffmann, *Acc. Chem. Res.* **1971**, *4*, 1.
- [7] B. Krijnen, H. B. Beverloo, J. W. Verhoeven, C. A. Reiss, K. Goubitz, D. Heijdenrijk, *J. Am. Chem. Soc.* **1989**, *111*, 4433.
- [8] W. Schuddeboom, T. Scherer, J. M. Warman, J. W. Verhoeven, *J. Phys. Chem.* **1993**, *97*, 13 092.
- [9] a) F. J. Hoogesteger, R. W. A. Havenith, J. W. Zwikker, L. W. Jenneskens, H. Kooijman, N. Veldman, A. L. Spek, *J. Org. Chem.* **1995**, *60*, 4375; b) F. J. Hoogesteger, Ph.D. Thesis, Utrecht University, Utrecht (The Netherlands), **1996**.
- [10] a) F. J. Hoogesteger, J. H. van Lenthe, L. W. Jenneskens, *Chem. Phys. Lett.* **1996**, *259*, 178; b) R. W. A. Havenith, J. H. van Lenthe, L. W. Jenneskens, F. J. Hoogesteger, *Chem. Phys.* **1997**, *225*, 139.
- [11] M. R. Wasielewski, M. P. Niemczyk, D. G. Johnson, W. A. Svec, D. W. Minsek, *Tetrahedron* **1989**, *45*, 4785.
- [12] a) H. Heitele, M. E. Michel-Beyerle, *J. Am. Chem. Soc.* **1985**, *107*, 8286; b) H. Heitele, M. E. Michel-Beyerle, P. Finckh, *Chem. Phys. Lett.* **1987**, *134*, 273.
- [13] a) F. J. Hoogesteger, J. M. Kroon, L. W. Jenneskens, E. J. R. Sudhölter, T. J. M. de Bruin, J. W. Zwikker, E. ten Grotenhuis, C. H. M. Marée, N. Veldman, A. L. Spek, *Langmuir* **1996**, *12*, 4760; b) F. J. Hoogesteger, L. W. Jenneskens, H. Kooijman, N. Veldman, A. L. Spek, *Tetrahedron* **1996**, *52*, 1773; c) E. ten Grotenhuis, J. P. van der Eerden, F. J. Hoogesteger, L. W. Jenneskens, *Chem. Phys. Lett.* **1996**, *250*, 549; d) E. ten Grotenhuis, J. P. van der Eerden, F. J. Hoogesteger, L. W. Jenneskens, *Adv. Mater.* **1996**, *8*, 666.
- [14] F. C. de Schryver, N. Boens, J. Put, *Adv. Photochem.* **1977**, *10*, 359.
- [15] T. Scherer, Ph.D. Thesis, University of Amsterdam, Amsterdam (The Netherlands), **1994**.
- [16] A. M. Brouwer, R. D. Mout, P. H. Maassen van den Brink, H. J. van Ramesdonk, J. W. Verhoeven, S. A. Jonker, J. M. Warman, *Chem. Phys. Lett.* **1991**, *186*, 481.
- [17] T. Scherer, W. Hielkema, B. Krijnen, R. M. Hermant, C. Eijkelhoff, F. Kerkhof, A. K. F. Ng, R. Verleg, E. B. van der Tol, A. M. Brouwer, J. W. Verhoeven, *Recl. Trav. Chim. Pays-Bas* **1993**, *112*, 535.
- [18] F. J. Hoogesteger, D. M. Grove, L. W. Jenneskens, T. J. M. de Bruin, B. A. J. Jansen, *J. Chem. Soc. Perkin Trans. 2* **1996**, 2327.
- [19] By using the described synthetic strategy, the synthesis of longer DA-substituted oligo(cyclohexylidenes) is straightforward.<sup>[9b]</sup>
- [20] H. Kooijman, A. L. Spek, F. J. Hoogesteger, L. W. Jenneskens, *Acta Crystallogr. Sect. C* **1997**, *53*, 1156.
- [21] a) J. B. Lambert, S. I. Featherman, *Chem. Rev.* **1975**, *75*, 611; b) C. H. Bushweller, S. H. Fleischman, G. L. Grady, P. McGoff, C. D. Rithner, M. R. Whalon, J. G. Brennan, R. P. Marcantonio, R. P. Domingue, *J. Am. Chem. Soc.* **1982**, *104*, 6224.
- [22] a) J. T. Gerig, *J. Am. Chem. Soc.* **1968**, *90*, 1065; b) F. R. Jensen, B. H. Beck, *J. Am. Chem. Soc.* **1968**, *90*, 1066.
- [23] P. Pasman, F. Rob, J. W. Verhoeven, *J. Am. Chem. Soc.* **1982**, *104*, 5127.
- [24] L. B. Krijnen, Ph.D. Thesis, University of Amsterdam, Amsterdam (The Netherlands), **1990**.
- [25] a) J. N. Murell, *J. Chem. Soc.* **1956**, 3779; b) K. Kimura, H. Tsubomura, S. Nagakura, *Bull. Chem. Soc. Jap.* **1964**, *37*, 1336.
- [26] Owing to its very limited solubility, it was not possible to quantitatively dissolve a known amount of **2DA** in cyclohexane. Therefore, the molar absorption coefficient of **2DA** was determined in dichloromethane (which is a better solvent). Thus, the spectrum of **2DA** in Figure 1 was taken in cyclohexane, but the molar absorption coefficient in dichloromethane was adopted. Although this makes a direct comparison with the spectra of the reference chromophores difficult, it is evident that no additional absorption peaks are present.
- [27] C. Reichardt, *Solvents and Solvent Effects in Organic Chemistry*, 2nd ed., VCH, Weinheim, **1988**.
- [28] R. M. Weiss, A. Warshel, *J. Am. Chem. Soc.* **1979**, *101*, 6131.

- [29] J. M. Warman, K. J. Smit, M. P. de Haas, S. A. Jonker, M. N. Paddon-Row, A. M. Oliver, J. Kroon, H. Oevering, J. W. Verhoeven, *J. Phys. Chem.* **1991**, *95*, 1979.
- [30] The Weller equation is given in Equation (1) below (A. Weller, *Z. Phys. Chem.* **1982**, *133*, 93). In this equation, the first term describes the half-wave redox potentials of the chromophores as determined in acetonitrile ( $\epsilon_s = 35.9$ ),<sup>[27]</sup> the second term the zero-zero excitation energy, the third term the Coulombic energy of the ion-pair separated by a distance  $R_{DA}$ , and the final term the solvation energy. The effective radii  $r_{d+}$  and  $r_{a-}$  of the radical cation and radical anion were obtained by using  $4\pi r^3/3 = M/N\rho$ , in which  $N$  is Avogadro's number,  $M$  is the molecular weight, and  $\rho$  the density of the compound. By using available data for *N,N*-dimethylaniline and tetracyanoethylene (*CRC Handbook of Chemistry and Physics*, 64th ed. (Ed.: R. C. Weast), CRC, Boca Raton, **1983**), values of 3.7 Å for  $r_{d+}$  and 3.4 Å for  $r_{a-}$  were obtained. Identical values were obtained for  $E_{1/2}^{ox}$  of **1D** and **2D** (0.70 V vs. SCE) and  $E_{1/2}^{red}$  of **1A** and **2A** (−1.70 V vs. SCE, see Experimental Section). For  $E_{00}$  the band edge of the lowest local transition was taken, which is situated at 317 nm (3.91 eV, Figure 1) for both **1DA** and **2DA**. The values for the donor–acceptor distance  $R_{DA}$  used, which were calculated with the molecular mechanics (MMX force field as implemented in PCMODEL 4.0, Serena Software, Bloomington, In., USA 1990) on extended conformations of the hydrocarbon skeleton, were 7.7 Å for **1DA** and 7.9 Å for **2DA**.
- $$\Delta G_{CS} = e(E_{1/2}^{ox} - E_{1/2}^{red}) - E_{00} - \frac{e^2}{4\pi\epsilon_0\epsilon_s R_{DA}} - \frac{e^2}{8\pi\epsilon_0} \left( \frac{1}{r_{d+}} + \frac{1}{r_{a-}} \right) \left( \frac{1}{35.9} - \frac{1}{\epsilon_s} \right) \quad (1)$$
- [31] R. M. Hermant, Ph.D. Thesis, University of Amsterdam, Amsterdam (The Netherlands), **1990**.
- [32] W. Schuddeboom, T. Scherer, J. M. Warman, J. W. Verhoeven, *J. Phys. Chem.* **1993**, *97*, 13 092.
- [33] R. J. Willemsse, Ph.D. Thesis, University of Amsterdam, Amsterdam (The Netherlands), **1997**.
- [34] M. R. Roest, J. M. Lawson, M. N. Paddon-Row, J. W. Verhoeven, *Chem. Phys. Lett.* **1995**, *230*, 536.
- [35] T. Clark, M. F. Teasley, S. Nelsen, H. Wynberg, *J. Am. Chem. Soc.* **1987**, *109*, 5719.
- [36] C. M. Previtali, *J. Photochem.* **1985**, *31*, 233.
- [37] T. Shida, *Electronic Absorption Spectra of Radical Ions, Physical Sciences Data, Vol. 34*, Elsevier, Amsterdam, **1988**.
- [38] M. P. de Haas, J. M. Warman, *Chem. Phys.* **1982**, *73*, 35.
- [39] W. Schuddeboom, Ph.D. Thesis, Delft University of Technology, Delft (The Netherlands), **1994**.
- [40] P. C. M. Weisenborn, C. A. G. O. Varma, M. P. de Haas, J. M. Warman, *Chem. Phys.* **1988**, *122*, 147.
- [41] S. P. McGlynn, T. Azumi, M. Kinoshita, *Molecular Spectroscopy of the Triplet State*, Prentice-Hall, Englewood Cliffs, **1969**.
- [42] N. J. Turro, *Modern Molecular Spectroscopy*, Benjamin/Cummings, Menlo Park, **1978**, p. 290.
- [43] C. A. van Walree, M. R. Roest, W. Schuddeboom, L. W. Jenneskens, J. W. Verhoeven, J. M. Warman, H. Kooijman, A. L. Spek, *J. Am. Chem. Soc.* **1996**, *118*, 8395.
- [44] D. F. Eaton, *Pure Appl. Chem.* **1988**, *60*, 1107.
- [45] J. Dachbach, D. Blackwood, J. W. Pons, S. Pons, *J. Electroanal. Chem.* **1987**, *237*, 269.
- [46] S. I. van Dijk, P. G. Wiering, C. P. Groen, A. M. Brouwer, J. W. Verhoeven, W. Schuddeboom, J. M. Warman, *J. Chem. Soc. Faraday Trans.* **1995**, *91*, 2107.

Received: June 29, 1999

Revised version: November 17, 1999 [F1879]